Accurate and general formalism for spin-mixing parameter calculations

Uday Chopra,[1,2] Shambhawi Shambhawi,[3] Sergei A. Egorov,[1,4,5] Jairo Sinova,[1] and Erik R. McNellis[1,*]

[1]*INSPIRE Group, Johannes Gutenberg University, Staudingerweg 7, D-55128 Mainz, Germany*

[2]*Graduate School Material Science in Mainz, Staudingerweg 9, D-55128 Mainz, Germany*

[3]*Department of Chemical Engineering and Biotechnology, University of Cambridge, Philippa Fawcett Dr, Cambridge CB30AS, United Kingdom*

[4]*University of Virginia, Chemistry Department, McCormick Rd, Charlottesville, Virginia 22901, USA*

[5]*Leibniz Institute for Polymer Research, Dresden, Hohe Strasse 6, D-01069 Dresden, Germany*

(Received 21 July 2019; published 8 October 2019)

The spin-admixture parameter γ is key to understanding spin dynamics in molecules. It measures the influence of spin-orbit coupling on spin dynamics in virtually all models for molecular materials. However, the predictive quality of its current first-principles electronic structure theory formulation [Z. G. Yu, Phys. Rev. B **85**, 115201 (2012)] is limited by multiple approximations. Consequently, current literature is lacking further first-principles predictions of γ beyond those of the original paper, and the application of such in computational studies of the role of spin mixing in organic and molecular spintronics. Here, we generalize the previous formulation of γ to remove all approximations limiting its predictive accuracy. The result is dramatic qualitative improvements in several model systems for organic spintronics. The significantly increased transferability of our method also allows its application to a range of heavier, metal-center "molecular qubit" molecules without modification. For these molecules, we identify molecular spin-orbit coupling as the key to their spin relaxation, with unprecedented accuracy. The accuracy and computational robustness of our reformulated method makes it ideal for the kind of large-scale, high-throughput computational exploration of chemical spaces used in several other areas of molecular nanotechnology.

DOI: 10.1103/PhysRevB.100.134410

I. INTRODUCTION

Molecular components and materials are a new dimension of the field of spintronics [1–3]. Their vast chemical tunability combined with rapid progress in molecular electronics, photonics, and magnetism fuels the interest in organic [1] and molecular [2] spintronics research. Applications currently range from, e.g., long spin lifetime applications in organic nanowires [4] and spin transport in high-mobility organic polymers [5,6], via hybrid organic-inorganic devices [7] and organic spin valves [8,9] to single-molecule magnets [10,11] and functionalized surfaces (so-called "spinterfaces" [12–14]).

Electronic structure calculations from first-principles theory have become an indispensable complement to experiments in these areas. Key to this success is a focus on properties difficult to measure, but that may be theoretically predicted with limited effort and consistent accuracy. In the following, we develop a previously established first-principles measure of molecular spin mixing into such a computing tool.

The ultimate goal of organic and molecular spintronics design is to tune molecular spin dynamics for a particular purpose. Electron spin relaxation (eSR) in molecular materials is (in the absence of photoexcitation and external magnetic fields) chiefly governed by a balance of major relaxation mechanisms, namely, (i) spin dipole and (ii) spin-exchange interactions, (iii) molecular hyperfine fields, (iv) spin-phonon coupling, and (v) electron scattering between mixed spin states. This balance depends on, e.g., the density and structural order of the material and its temperature and charge density, in addition to single-molecule properties. Spin dipole interactions are weak and short ranged, and therefore often negligible in disordered soft matter. Spin-exchange couplings are similarly often weak and short ranged in molecules. Spin exchange as such does not relax spin, but may enhance relaxation by other mechanisms. Hyperfine field relaxation depends on field strength and spin dwell time at a molecule.

In spin-phonon coupling, the spin-orbit coupling (SOC) of the molecular spin to the opposite polarization may allow for thermal relaxation, if the phonon density of states in the system is sufficient to absorb the resulting Zeeman energy difference [15–18]. SOC also gives rise to mixing of spins in electronic states. Momentum scattering between such mixed states, the so-called Elliott-Yafet (EY) mechanism [19,20], is the main cause of spin relaxation in traditional semiconductors. SOC similarly mixes molecular spins [21]. In an organic or molecular semiconductor characterized by hopping charge transport, *spatial* scattering between mixed spin states therefore works in direct analogy to, and with equal importance for, spin dynamics as EY relaxation.

Spin mixing in these scattering states is often weak, and correspondingly well described perturbatively in SOC. The first-order perturbation correction to the spin-free Hamiltonian, that is, the spin admixture parameter γ, has been derived for crystalline semiconductors [19,20], molecules [21],

*emcnelli@uni-mainz.de

and, more recently, for molecular electronic structure theory [22,23]. The ratio of spin-flipping to spin-conserving charge hops in a molecular semiconductor is directly proportional to γ^2 [23].

Despite the fact that γ has become a vital parameter in a range of influential molecular spin dynamics models [22–24], and a central concept for current experimental [25–30] and theoretical [31–37] molecular spintronics, no further attempts to calculate or analyze γ from first-principles theory have been made, likely because of the significant methodological limitations of its current formulation [23]. In this formulation, calculations of γ are restricted to π orbitals in organic molecules and a wave-function quality below current standards of electronic structure modeling.

This paper consists of three main parts. First, in Sec. II A we generalize γ to remove all limitations on predictive accuracy and transferability between different systems inherent in the original formulation [23]. Second, we study the performance of our method in the same model systems examined using the original formulation, while exploring the influence of electronic exchange-correlation approximations on γ, as described in Sec. II B. These light organic molecules are primarily relevant to organic spintronics. Here, our reformulated γ recovers important spin physics lost in the original method. Third, we gauge the accuracy and emphasize the transferability of our method by explaining the variation in spin relaxation rates in a series of metal-phthalocyanine (MPc) molecules, molecular "qubits," measured by Bader *et al.* [38] These molecules are relevant to molecular spintronics, and too complex for the original method. This experiment is designed such that all but SOC effects of the above-mentioned spin relaxation mechanisms cancel. Therefore, the correlation between measured eSR rates and calculated γ is a measure of the accuracy of the SOC approximation of the latter. While our calculations alone do not allow for the prediction of such eSR rates, the similarity of variation between the two is testament to the accuracy of our method, which as a first-principles quantity should hold for a wide range of similar molecules. All results and a discussion of the same are presented in Sec. III, while the key points of this work are summarized in Sec. IV.

II. THEORY

A. Generalization of spin-admixture parameter

We begin by generalizing the first-principles formulation of γ from the previous derivation of Ref. [23]. The dominant single-electron term of the Breit-Pauli [39,40] SOC operator is in atomic units

$$\hat{H}_{\mathrm{SOC}} = \frac{\alpha^2}{2}\sum_{i,k}\left(\frac{Z_k}{r_{ik}^3}\hat{\mathbf{r}}_{ik}\times\hat{\mathbf{p}}_i\right)\cdot\hat{\mathbf{s}}_i = \frac{\alpha^2}{2}\sum_i \xi_i\hat{\mathbf{l}}_i\cdot\hat{\mathbf{s}}_i$$
$$= \frac{\alpha^2}{4}\sum_i \xi_i\begin{bmatrix}\hat{\mathbf{l}}_i^z & \hat{\mathbf{l}}_i^- \\ \hat{\mathbf{l}}_i^+ & -\hat{\mathbf{l}}_i^z\end{bmatrix},\ \hat{\mathbf{l}}^{+(-)} = \hat{\mathbf{l}}^x + (-)i\hat{\mathbf{l}}^y, \quad (1)$$

where α is the fine-structure constant, $\hat{\mathbf{r}}_{ik}$ is the separation vector to atomic nucleus k of effective charge Z_k, $\hat{\mathbf{p}}_i$ is the momentum, and $\hat{\mathbf{s}}_i$ is the spin angular momentum for the ith electron. The spin-orbit (SO) constants ξ_i provide the nuclear Coulomb potential scaling of orbital angular momentum $\hat{\mathbf{l}}_i$ relative to the atomic nuclei for electron i. In the last step, $\hat{H}_{\mathrm{SOC}}$ is written in the Pauli spin basis. Expectation values of $\hat{\mathbf{l}}^z$ ($\hat{\mathbf{l}}^{+/-}$) are nonzero for orbital pairs of same (opposite) spin.

The first-order perturbation correction due to $\hat{H}_{\mathrm{SOC}}$ is the change in the norm from normalized, SO-free, pure-spin molecular orbitals (MOs) $|\psi\uparrow\rangle$ to perturbed, mixed quasispin orbitals $|\psi+\rangle$ [23] (equivalently for $|\psi\downarrow\rangle/|\psi-\rangle$):

$$\langle\psi_0+|\psi_0+\rangle = \langle\psi_0\uparrow|\psi_0\uparrow\rangle + \gamma^2 = 1 + \gamma_{\uparrow\uparrow}^2 + \gamma_{\uparrow\downarrow}^2, \quad (2)$$

where γ^2 is the sum of mixing between same ($\gamma_{\uparrow\uparrow}^2$) and opposite ($\gamma_{\uparrow\downarrow}^2$) spin orbitals, arising from the $\hat{\mathbf{l}}^z$ and $\hat{\mathbf{l}}^{+/-}$ operators, respectively. The subscript 0 indexes the spin-carrying orbital.

Reference [23] calculates $|\psi\uparrow\rangle$ from density-functional theory (DFT), and constructs $|\psi_0+\rangle$ within the restricted open-shell Kohn-Sham (ROKS) approximation as

$$|\psi_0+\rangle = |\psi_0\uparrow\rangle - \sum_{k\neq 0\sigma}\frac{\langle\psi_k\sigma|\sum_i\xi_i\hat{\mathbf{l}}_i\cdot\hat{\mathbf{s}}_i|\psi_0\uparrow\rangle}{E_k - E_0}|\psi_k\sigma\rangle$$
$$= |\psi_0\uparrow\rangle - \sum_{k\neq 0}\frac{1}{2}\left[\frac{\langle\psi_k\uparrow|\sum_i\xi_i\hat{\mathbf{l}}_i^z|\psi_0\uparrow\rangle}{E_k - E_0}|\psi_k\uparrow\rangle\right.$$
$$\left. - \frac{\langle\psi_k\downarrow|\sum_i\xi_i\hat{\mathbf{l}}_i^-|\psi_0\uparrow\rangle}{E_k - E_0}|\psi_k\downarrow\rangle\right], \quad (3)$$

where $|\psi_k\rangle$ are the orbitals of the SO-free Hamiltonian, and E_k are the corresponding orbital energies obtained from ROKS electronic structure calculations. σ and i are summations over spins and orbitals, respectively. The ROKS approximation represents a very significant variational constraint on the Kohn-Sham wave function compared to the unrestricted (UKS) approximation.

At this point, Ref. [23] approximates the unknown SO constants ξ_i by mapping experimental measurements of atomic orbitals (AOs) up to p angular momentum onto the matrix elements of Eq. (3), which is only possible with a basis set of one function per canonical AO, that is, a minimal basis set. Besides semiempiricity, this implies further severe variational restrictions on the molecular wave function, in addition to those imposed by the ROKS approximation. While in principle expandable to higher angular momentum AOs, the limitation to p basis functions also restricts the technique to calculations on molecular π orbitals and consequently, to light organic molecules only.

We begin our modifications by generalizing Eq. (3) to the UKS approximation. Following Neese and Solomon [41], this is achieved by simply spin labeling the eigenvalue in the denominator of Eq. (3) ($E_k \rightarrow E_{k\uparrow}\,/\,E_{k\downarrow}$), and using the UKS in the electronic structure calculation.

Next, we address the SOC approximation using the zeroth-order regular approximation [42] (ZORA) to the fully relativistic Dirac equation [43]. The idea is to calculate SOC matrix elements from first-principles theory, and apply them to the same level of theory excluding the SOC. The full ZORA Hamiltonian is $\hat{\mathrm{H}}^{\mathrm{ZORA}} = \hat{\mathrm{H}}_{\mathrm{SR}}^{\mathrm{ZORA}} + \hat{\mathrm{H}}_{\mathrm{SO}}^{\mathrm{ZORA}}$, where

$$\hat{\mathrm{H}}_{\mathrm{SR}}^{\mathrm{ZORA}} = V + \hat{\mathbf{p}}\frac{c^2}{2c^2 - V}\hat{\mathbf{p}}$$
$$\text{and } \hat{\mathrm{H}}_{\mathrm{SO}}^{\mathrm{ZORA}} = \frac{c^2}{(2c^2 - V)^2}\hat{\mathbf{s}}\cdot(\nabla V\times\hat{\mathbf{p}}), \quad (4)$$

where V is the total electronic potential (the sum of nuclear, electronic, and exchange-correlation potentials), and the scalar-relativistic Hamiltonian $\hat{H}_{SR}^{ZORA}$ excludes the SO term.

The spatial matrix elements of $\hat{H}_{SO}^{ZORA}$ in the Pauli spin basis are [42]

$$\hat{L}_{ij}^{l} = i \sum_{mn} \epsilon_{lmn} \left\langle \frac{\partial \psi_i}{\partial x_m} \middle| \frac{V}{4c^2 - 2V} \middle| \frac{\partial \psi_j}{\partial x_n} \right\rangle, \tag{5}$$

where the permutation matrix ϵ_{lmn} is the Levi-Civita tensor and x_m is the Cartesian basis. We note that the matrix elements $\hat{L}_{ij}^{l}$ by way of V are scaled by effective SO constants, inheriting the first-principles qualities of V.

We transform these matrix elements to the MO basis, and substitute them into Eq. (3), with the important difference from Ref. [23], that the MOs $|\psi\rangle$ are calculated using the scalar-relativistic ZORA. We write the mixed spin-carrying orbital as

$$|\psi_0 +\rangle = |\psi_0 \uparrow\rangle + \sum_{k\neq 0} [a_k |\psi_k \uparrow\rangle + b_k |\psi_k \downarrow\rangle], \tag{6}$$

where

$$a_k = \frac{1}{2} \frac{\langle \psi_k \uparrow | \hat{L}^z | \psi_0 \uparrow \rangle}{E_{k\uparrow} - E_0}$$

$$\text{and} \quad b_k = \frac{1}{2} \frac{\langle \psi_k \downarrow | (\hat{L}^x + i\hat{L}^y) | \psi_0 \uparrow \rangle}{E_{k\downarrow} - E_0}. \tag{7}$$

Here, $\hat{L}^{x,y,z}$ are the full matrices of Eq. (5). Note the spin-labeled eigenvalues ($E_{k\downarrow}$ / $E_{k\uparrow}$) for UKS.

Finally, substituting Eq. (7) into Eq. (6), and further into Eq. (2), we obtain

$$\gamma^2 = \sum_{k\neq 0} [a_k^* a_k + b_k^* b_k] \tag{8}$$

for the spin-mixing parameter γ of the UKS/scalar-relativistic ZORA ground state, where we note that γ^2 is proportional to the square of the SOC matrix elements [Eq. (5)].

This generalization eliminates the orbital angular momentum and basis set restrictions of the previous formulation, allowing for well-converged all-electron calculations of γ in any orbital of any molecule for which the ZORA is valid. The ZORA is valid for any single-determinantal level of theory with electronic interactions described by an effective potential V. While it would be straightforward to rederive γ for a more sophisticated scalar-relativistic/two-component approximation (such as the Douglas-Kroll-Hess family [44,45]), the quality of V is in our estimation the greater source of error.

B. Density-functional theory calculations

The quality of the effective electronic potential affects γ in two ways, namely, via the SOC matrix elements, and the spatial and energetic density of states (DOS), i.e., the orbital overlaps and eigenvalue energy differences in the numerator and denominator of Eq. (7), respectively. A consistently high quality of V across different kinds of molecules is synonymous with accuracy and transferability of γ.

Because of the so-called electron delocalization error [46], the DOS of molecules is often poorly described by (semi)local DFT exchange-correlation (xc) functionals, leading to substantial errors in molecular properties [47]. So-called hybrid xc functionals canceling some delocalization error by the addition of "exact" nonlocal Hartree-Fock exchange have proven a successful solution to this problem, from calculations of electronic [47] and magnetic [48,49] properties in organic molecules to light transition metal chemistry [49,50].

We here systematically quantify the influence of (semi)local xc approximations on the calculation of γ. Starting from the semilocal Perdew-Burke-Ernzerhof (PBE) [51] generalized gradient approximation (GGA) xc functional employed in Ref. [23] for reference, we compare to calculations using the same functional with 25% exact exchange, the so-called PBE0 [52] hybrid xc functional. We also study the strictly nonlocal, 100% exact exchange Hartree-Fock (HF) approximation. For comparison with a strictly local xc approximation, we also include the local density approximation (LDA) functional forming the main component of PBE, which is commonly labeled PW92 [53].

While (as already demonstrated by some of us [5]) PBE0 yields accurate γ, electron delocalization error is not the only limitation of DFT as commonly applied of potential importance for future γ calculations. The so-called static correlation error [46] leads to large errors in properties of systems with near-degenerate, strongly correlated states, such as in high-angular-momentum semicore states of heavier (f-electron) transition elements. *Prima facie*, this limits the applicability of any DFT-based method to, e.g., lanthanide single-molecule magnets (SMMs) [10,11]. While such systems are outside the scope of this work, we wish to highlight the successes of range-separated hybrid functionals in this area. The range-separated version of PBE0, the so-called HSE [54,55] functional, performs excellently for electronic [54] and magnetic [56] properties of lanthanide compounds, even solids [57] In short, we remain confident that the high predictive accuracy of our γ formulation will remain well outside the scope of the systems studied here if (a) spin mixing remains sufficiently weak for a low-order perturbation treatment, and (b) the xc-functional approximation is chosen judiciously.

We use the NWCHEM quantum chemistry suite [58] version 6.5 for all DFT calculations within the zeroth-order regular approximation (ZORA). All properties were found converged with respect to the SARC [59] all-electron, minimally augmented, polarized triple-zeta valence basis set recontracted for ZORA (that is, "MA-ZORA-Def2-TZVP"). This basis set, with the carbon atom diffuse (minimal augmentation) functions removed in order to eliminate linear dependencies, was used in all calculations unless otherwise stated.

Because of the partially very weak spin mixing in the studied molecules, great care was taken to eliminate sources of numerical errors in the calculations: the self-consistent field (SCF) convergence and Coulomb integral screening thresholds were set at $10^{-8} - 10^{-10}$ Ha and 10^{-14}, respectively. Integration grids were set at the maximum ("xfine") density. SCF convergence aids such as level shifting, and initial high tolerances in the SCF cycle were turned off (options "no level shifting" and "tight," respectively). Spin contamination was negligible ($<$10%) in all UKS calculations.

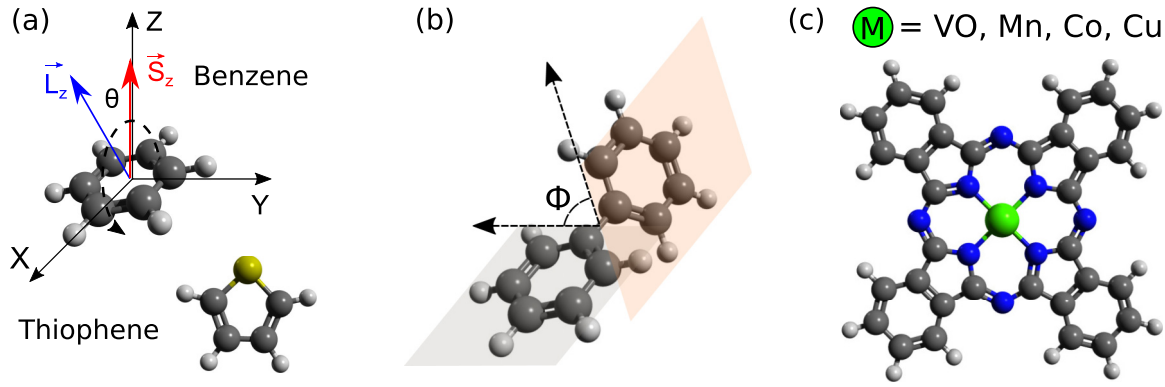

FIG. 1. (a) Benzene (C_6H_6) and thiophene (C_4H_4S) molecules, with an illustration of the rotation of their conjugation plane with fixed spin quantization axis. (b) Biphenyl ($C_{12}H_{10}$) with the definition of the phenyl ring dihedral angle. (c) Metal-phthalocyanine (MPc, $C_{32}H_{16}\,\mathbf{M}\,N_8$).

Hyperfine field strengths were calculated using the method of Ref. [60] from standard hyperfine coupling calculations at the same level of theory used for the spin-mixing calculations.

The lighter, closed-shell molecules studied are nonmagnetic, and only exhibit spin mixing as ions. These charged molecules were calculated in doublet ground states. The magnetic MPc molecules were left charge neutral, and calculated in multiplicities of 2 for VO, Co, and Cu, and 4 for Mn. All γ calculations were done on molecules fully geometry optimized in the respective charge states, at the stated level of theory, without symmetry constraints.

The scripts necessary for the calculation of the reformulated γ from the output of an NWCHEM ZORA/DFT calculation may be downloaded online.[1]

III. RESULTS AND DISCUSSION

A. Benzene

We begin by computing our reformulated γ in several model systems first studied in Ref. [23]. In order to study the effects on our generalized γ of the relative orientation of orbital and spin angular momentum, we rotate the spin in a planar orbital. The highest occupied molecular orbital (HOMO) of benzene (C_6H_6), which has p_z orbital angular momentum, is the simplest possible such system. We add a single positive charge (electron hole) to benzene, and rotate the molecule by an angle θ through 180° about the y axis, with the spin quantization axis fixed along z, which is equivalent to rotating the spin in a stationary molecule from parallel to antiparallel alignment with the orbital angular momentum [see Fig. 1(a)].

We first isolate the effect of the unrestricted Kohn-Sham (UKS) vs restricted open-shell Kohn-Sham (ROKS) approximations on γ, using the PBE xc functional, the "STO-6G" Slater-type minimal basis set, and the SOC approximation and empirical ξ_i as in Ref. [23]. This is shown in Fig. 2. Our ROKS results are quantitatively very close and qualitatively identical to those of Ref. [23]. The ROKS γ^2 (blue solid line) is constant with the rotation angle θ. The reason is the orbital symmetry of the ROKS canceling the changes in the opposite- ($\gamma^2_{\uparrow\downarrow}$, dashed blue line) and same-spin ($\gamma^2_{\uparrow\uparrow}$, dotted blue line) contributions to γ^2. This is obviously incorrect since properties proportional to the absolute magnitude squared of the $\hat{\mathbf{l}}\cdot\hat{\mathbf{s}}$ scalar product [Eq. (1)] should follow a $\cos^2(\theta)$ curve.

Repeating the calculation using the UKS approximation (solid red line), this is indeed what we find, albeit weakly for benzene. The benzene SOC, and therefore γ^2 is small, and so is its variation with θ. In order to rule out mere numerical artifacts, we repeat the calculation for thiophene [C_4H_4S, see Fig. 1(a)], which has stronger SOC. The resulting identical but much stronger effect on γ^2 is shown in the magenta curve in Fig. 2. The reason for this variation is the UKS orbital asymmetry reducing $\gamma^2_{\uparrow\downarrow}$ more than the increase in $\gamma^2_{\uparrow\uparrow}$ around $\theta = 90°$. The thiophene $\gamma^2_{\uparrow\downarrow}$ and $\gamma^2_{\uparrow\uparrow}$ curves differ from those of benzene in magnitude only, and have been left out of Fig. 2 for clarity.

Next, we examine the effect of electron delocalization error on the benzene $\gamma^2(\theta)$ curves, by recomputing with the above

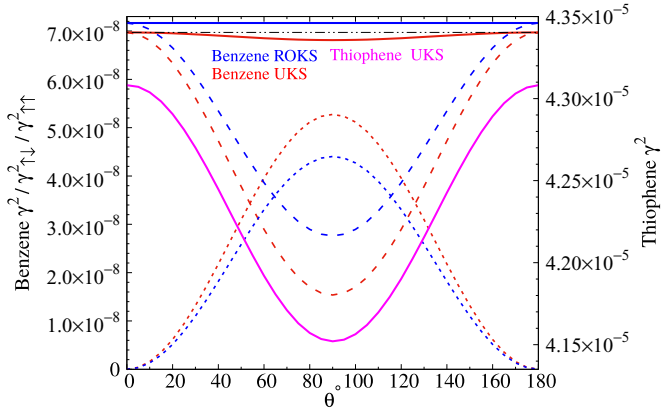

FIG. 2. Variation of γ^2 with rotation of conjugation plane relative to the spin quantization axis (see Fig. 1). Left y axis: ROKS (blue) and UKS (red) results for benzene. Solid, dotted, and dashed lines represent γ^2, $\gamma^2_{\uparrow\uparrow}$, and $\gamma^2_{\uparrow\downarrow}$, respectively. Note the UKS (ROKS) asymmetry (symmetry) of $\gamma^2_{\uparrow\uparrow}$ and $\gamma^2_{\uparrow\downarrow}$. Right y axis: UKS curve for thiophene (magenta). The thiophene $\gamma^2_{\uparrow\downarrow}$ and $\gamma^2_{\uparrow\uparrow}$ curves differ from benzene in magnitude only, and have been left out for clarity.

[1] https://github.com/UdayChopra/spin-admixture

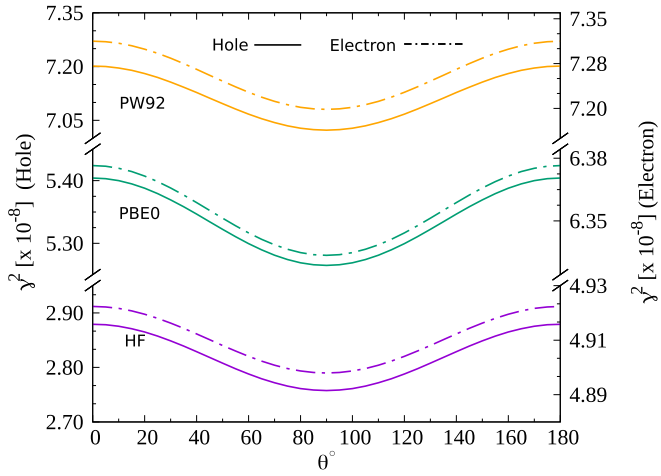

FIG. 3. The UKS γ^2 curve of Fig. 2 repeated for fully local (PW92), hybrid (PBE0), and fully nonlocal (HF) xc approximations for cationic (solid line) and anionic (dotted-dashed line) benzene molecules.

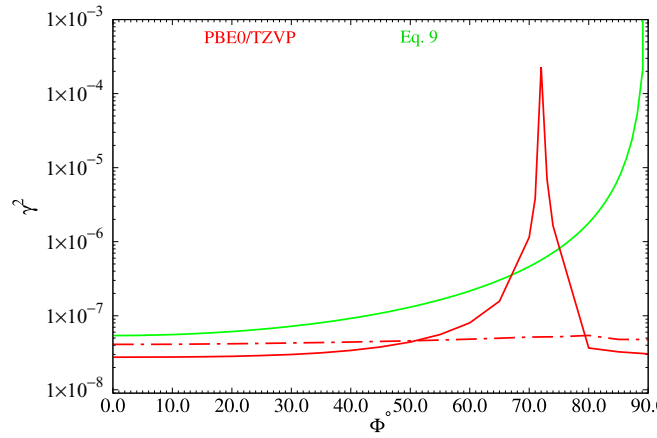

FIG. 4. γ^2 as a function of dihedral torsion in a biphenyl molecule at ZORA/UKS/PBE0/TZVP level of theory (red) compared with Eq. (9) (green). Solid (dashed) lines indicate positive (negative) biphenyl ions.

level of theory, but different exchange-correlation (xc) approximations (see Fig. 3). The $\gamma^2(\theta)$ curves stay qualitatively the same, but quantitatively reduce by almost a factor of 3 from a fully local (LDA/PW92) via a hybrid (PBE0) to a fully nonlocal (Hartree-Fock, HF) xc approximation, for both positive (solid lines) and negative charges (dashed lines). The LDA curve in Fig. 3 is nearly identical to that of GGA/PBE in Fig. 2. The high γ for the (semi)local functionals is due to underestimated orbital energy differences in the denominator of Eq. (7), caused by electron delocalization error. However, since the HF approximation induces the opposite error [46]. the best estimate of γ lies between the LDA/GGA and HF extremes. Therefore, while the exact solution is unknown, the hybrid PBE0 xc functional is closest to it.

From here on, we employ the ZORA/UKS/PBE0 level of theory with a TZVP basis set (see Sec. II B) in all calculations. In the simple benzene system, the only effect of this improvement is an overall shift of the curves in Figs. 2 and 3.

B. Biphenyl

Reference [23] saliently points out that the spin mixing in a conjugated molecule depends on the angle Φ between adjacent π-orbital planes. This is key to the variation of spin mixing with structure in, e.g., high-mobility polymers, and therefore of great importance to organic spintronics [61].

In a fictitious system of two adjacent, identical π orbitals, only $\gamma^2_{\uparrow\uparrow}$ depends on Φ, leading to the expression

$$\gamma^2(\Phi) = \frac{\xi^2}{2\Delta^2}\left[1 + \frac{1}{8}\tan^2(\Phi)\right], \tag{9}$$

where ξ is the equivalent SO constant for both orbitals, and Δ is the π-σ orbital energy difference. The orbitals are assumed not to change with Φ. Equation (9) is a reasonable approximation of the original (ROKS) γ^2 as a function of the dihedral angle Φ between the phenyl ring planes, in both positively and negatively charged biphenyl molecules [23] [see Fig. 1(b)].

We also study this system for comparison. Figure 4 shows our ZORA/UKS/PBE0/TZVP $\gamma^2(\Phi)$ curves of the positive and negative biphenyl ions compared to Eq. (9). While the curve for the positive ion is in similar agreement with Eq. (9) as the original γ^2 [23], the reformulated γ^2 is nearly constant with Φ in the negative ion. This is simply because the electronic structure as a function of molecular distortion is a complex, nonlinear balance between electronic and geometric effects, that may differ greatly between molecules, orbitals, and charge states. The resulting spin mixing is significantly better described by our reformulated γ. For example, in our calculations both $\gamma^2_{\uparrow\downarrow}$ and $\gamma^2_{\uparrow\uparrow}$ vary strongly with Φ, proving that while Eq. (9) provides essential qualitative insight, it is too simplistic for quantitative evaluation. The predictive accuracy of our reformulated γ for structural variations in high-mobility organic polymers has already been demonstrated elsewhere [5].

C. Metal-phthalocyanines

The physics of the reformulated γ are undeniably improved when compared to theoretical calculations on light organic molecules. Still, a comparison to experiments on the complex, heavy, magnetic molecules relevant for molecular spintronics is more convincing of the accuracy and transferability of the new method. Because γ is not an experimental observable, and its influence on spin relaxation generally obscured in a complicated balance of mechanisms, such a comparison is difficult. Beyond already demonstrated improvements, the key factor in the accuracy of γ is that of the SOC approximation. We therefore reduce our focus to the *correlation* between theoretical γ and SOC dominated, experimentally measured spin relaxation rates, rather than trying to predict the latter from first principles.

Metal-center molecules are highly relevant for molecular spintronics [2,62]. Bader *et al.* [38] have measured the longitudinal spin relaxation time T_1 of metal-phthalocyanine (MPc) molecules, prototypical molecular qubits [38,63,64] [see Fig. 1(c)]. The MPcs, where M are the 2+ ions of VO

TABLE I. From left to right: the spin-carrying orbital in the four MPc molecules (see text), the calculated γ^2 value of these orbitals, the inverse of T_1 for each MPc measured in D_2SO_4 solution at 7 K [38], and the error to experiment of T_1 approximated on the form $T_1 \approx \frac{\kappa}{\gamma^2}$ (see text).

Orbital	γ^2	$(T_1)^{-1}$ (MHz) [38]	T_1 Fit error (%)
VOPc (d_{xy})	6.20×10^{-6}	4.16×10^{-7}	+16
MnPc (d_{yz}/d_{zx})	2.41×10^{-2}	1.45×10^{-3}	+5
CoPc (d_{z^2})	5.70×10^{-3}	9.01×10^{-5}	−61
CuPc ($d_{x^2-y^2}$)	3.72×10^{-4}	9.71×10^{-6}	−55

(vanadyl) Mn, Co and Cu, are dissolved in D_2SO_4 solutions at 7 K. These MPcs are paramagnetic because of odd occupancy of the metal center d shells.

As described in the Introduction, five major spin relaxation mechanisms contribute to T_1. The influence of spin dipole interactions is negligible in a disordered system like a frozen MPc solution. The disorder also virtually eliminates spin exchange, which is already weak in highly ordered thin films of these molecules [65,66]. Since their nuclear spin distribution only differs at the metal center, the hyperfine field (HF) relaxation contribution is similar in all four MPcs, and does not contribute to the variation in T_1. We verified this by calculating the effective HF in each molecule from hyperfine couplings [60] computed at the same level of theory as γ. The VO, Co, and CuPc HF strengths are indeed near identical at 39, 34, and 37 mT, respectively. While the MnPc HF strength is lower at 13 mT, this does not explain the order of magnitude variation in measured spin relaxation rates. Hopping charge transfer, while physically possible, is likely negligible at 7 K. To the extent that it does occur, its electron spin relaxation (eSR) rate contribution is proportional [23] to the hopping frequency times γ^2, i.e., the SOC matrix elements squared [see Eq. (8)].

Thermal spin relaxation via spin-phonon coupling is a strong, complex effect in similar metal-center molecules [64,67]. Bader *et al.* also identify this as the main spin relaxation mechanism in the MPc series. However, they do not attribute the variation in measured T_1 to SOC since it does not correlate with the atomic SOC strength of the metal center, with the Cu T_1 [rate $(T_1)^{-1}$] significantly longer (lower) than that of Mn.

Importantly, whether spin-phonon coupling occurs with the relaxation energy absorbed by a molecular vibron (so-called intramolecular eSR [68,69]), or as a single-phonon or multiphonon process, the spin-phonon and Elliott-Yafet analog eSR mechanisms depend identically on SOC [$\propto(\hat{H}_{SO})^2$] [15–18]. We therefore make the ansatz, that the aggregate rate $(T_1)^{-1} \propto \gamma^2$, and fit the data of Table I on the form $\gamma^2 T_1 \approx \kappa$.

See the correlation plot in Fig. 5. A fit of $\kappa = 1.73 \times 10^{-5}$ s produces relaxation times $T_1 \approx \frac{\kappa}{\gamma^2}$ with an RMS error of ∼40% compared to experiment, over four orders of magnitude (see Table I). First, this high correlation is in striking support of molecular SOC as the explanation for the variation in T_1 in the experiment by Bader *et al.* [38]. Second, the only technical difference between these and the above calculations on simple, nonmagnetic organic molecules is a change in the index of the spin-carrying orbital, which is a similarly striking testament to the accuracy and transferability of our method, and very promising for its application to a wider range of molecules. Since MPcs are too complex for the original formulation of γ, Ref. [23] resorts to ligand field theory to obtain $\gamma^2 = 6.80 \times 10^{-4}$ for the CuPc $d_{x^2-y^2}$ orbital, similar to our first-principles result.

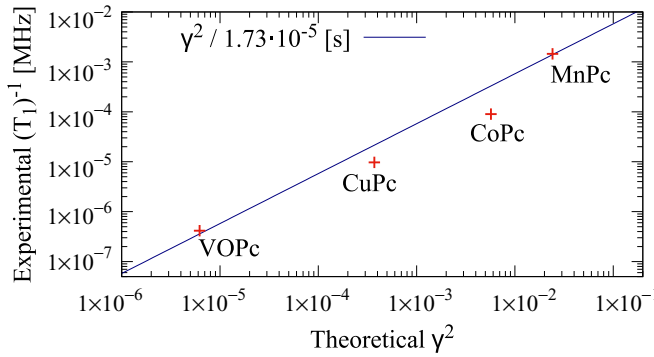

FIG. 5. Correlation plot of γ^2 vs aggregate spin relaxation rates $(T_1)^{-1}$ for the four MPc molecules, and a linear fit on the form $(T_1)^{-1} = \frac{\gamma^2}{\kappa}$ (see text).

IV. SUMMARY

Despite spin mixing having a major influence on the spin dynamics in molecular semiconductor materials, first-principles calculations of the spin-mixing parameter γ have yet to serve the organic and molecular spintronics fields. We have generalized the previous formulation of γ, removing detrimental simplifications, and raising its predictive accuracy to one limited only by the underlying wave function and SOC approximations. Choosing a hybrid DFT exchange-correlation functional and the ZORA for the latter, respectively, combines a reduced electron delocalization error and nonempirical SOC matrix elements with significantly reduced wave-function constraints implied by a free choice of basis sets and the unrestricted Kohn-Sham approximation.

For convenience, Table II shows a direct comparison of all γ^2 computed both here and in Ref. [23]. In the light organic molecules, our values differ between little in the benzene cation, to approximately a factor of 3 in the biphenyl

TABLE II. Comparison of all γ^2 calculated here, and also found in Ref. [23]. *Value obtained by ligand-field theory, rather than a direct first-principles calculation.

Molecule (orbital)	Total charge	γ^2 This work	γ^2 Ref. [23]
Benzene (p_z)	+1	5.40×10^{-8}	5.46×10^{-8}
	−1	6.38×10^{-8}	1.32×10^{-7}
Biphenyl (p_z)	+1	2.75×10^{-8}	5.22×10^{-8}
	−1	4.10×10^{-8}	1.18×10^{-7}
CuPc ($d_{x^2-y^2}$)	0	3.72×10^{-4}	$^*6.80 \times 10^{-4}$

anion. However, this static geometry comparison obscures the improvement in the dependence of the reformulated γ on spin polarization relative to molecular electronic structure in conjugated molecules. This improvement is also evident in the richer and more complex (yet, as proven, more accurate [5]) dependence of γ on the angles between adjacent π orbitals. The latter finding also emphasizes the qualitative differences between γ of positively and negatively charged such molecules, consistent with the differences in their electronic structure. Table II also shows our γ^2 value for copper-phthalocyanine, obtained in a manner identical to those of the light-conjugated molecules, in contrast to Ref. [23], which is unable to treat transition metal elements from first principles, and consequently resorts to a ligand-field theory calculation.

The strong correlation between our theoretically predicted γ in the metal-phthalocyanine series and their experimentally measured aggregate longitudinal spin relaxation rates is testament to the strong dependence on molecular SOC of the latter, and the accuracy and transferability of the ZORA for this property. Importantly, this result is achieved without manual input or analytical derivations in special cases, and computationally robust, standard electronic structure theory eminently suitable for large-scale computation. We therefore finally highlight our reformulation as an ideal tool for future so-called high-throughput computational studies in organic and molecular spintronics.

In high-throughput computation as used in, e.g., organic photovoltaics [70] and battery research [71], a highly automatable and consistently accurate theoretical method is used to scan properties of a whole class of molecules, allowing for resource-efficient exploration of chemical spaces and, correspondingly, efficient exploitation of chemical tunability. In a recent publication [6], we have used our reformulation to obtain a statistical picture of γ in every charged electronic state of a mesoscale organic polymer model, amounting to hundreds of DFT calculations on long polymer chains. In a similar vein, we have used our method in another recent publication [72] to describe trends throughout several molecule classes relevant for organic and molecular spintronics.

ACKNOWLEDGMENTS

Invaluable discussions with and computer code shared by Dr. Z. G. Yu are most gratefully acknowledged. Funding from the Alexander von Humboldt Foundation, the ERC Synergy Grant SC2 (No. 610115), the Transregional Collaborative Research Center (SFB/TRR) 173 SPIN+X, and Grant Agency of the Czech Republic Grant No. 14-37427G is acknowledged. U.C. is a recipient of a DFG-funded position through the Excellence Initiative by the Graduate School Materials Science in Mainz (GSC 266).

[1] Z. V. Vardeny, S. Majumdar, H. Majumdar, R. Österbacka, and Z. V. Vardeny, *Organic Spintronics*, edited by Z. Vardeny, Vols. 1–5 (CRC Press. Boca Raon, FL, 2010). pp. 1–335.
[2] S. Sanvito, Chem. Soc. Rev. **40**, 3336 (2011).
[3] A. Cornia and P. Seneor, Nat. Mater. **16**, 505 (2017).
[4] S. Pramanik, C. G. Stefanita, S. Patibandla, S. Bandyopadhyay, K. Garre, N. Harth, and M. Cahay, Nat. Nanotechnol. **2**, 216 (2007).
[5] S.-J. Wang, D. Venkateshvaran, M. R. Mahani, U. Chopra, E. R. McNellis, R. Di Pietro, S. Schott, A. Wittmann, G. Schweicher, M. Cubukcu, K. Kang, R. Carey, T. J. Wagner, J. N. M. Siebrecht, D. P. G. H. Wong, I. E. Jacobs, R. O. Aboljadayel, A. Ionescu, S. A. Egorov, S. Mueller *et al.*, Nat. Electron. **2**, 98 (2019).
[6] S. Schott, U. Chopra, V. Lemaur, A. Melnyk, Y. Olivier, R. Di Pietro, I. Romanov, R. L. Carey, X. Jiao, C. Jellett, M. Little, A. Marks, C. R. McNeill, I. McCulloch, E. R. McNellis, D. Andrienko, D. Beljonne, J. Sinova, and H. Sirringhaus, Nat. Phys. **15**, 814 (2019).
[7] V. A. Dediu, L. E. Hueso, I. Bergenti, and C. Taliani, Nat. Mater. **8**, 707 (2009).
[8] J. Devkota, R. Geng, R. C. Subedi, and T. D. Nguyen, Adv. Funct. Mater. **26**, 3881 (2016).
[9] G. Cucinotta, L. Poggini, A. Pedrini, F. Bertani, N. Cristiani, M. Torelli, P. Graziosi, I. Cimatti, B. Cortigiani, E. Otero, P. Ohresser, P. Sainctavit, A. Dediu, E. Dalcanale, R. Sessoli, and M. Mannini, Adv. Funct. Mater. **27**, 1703600 (2017).
[10] L. Bogani and W. Wernsdorfer, in *Nanoscience Technology*, edited by Peter Rodgers (Nature Publishing Group) (Copublished with Macmillan, UK, 2009), pp. 194–201.
[11] D. N. Woodruff, R. E. P. Winpenny, and R. A. Layfield, Chem. Rev. **113**, 5110 (2013).
[12] S. Sanvito, Nat. Phys. **6**, 562 (2010).
[13] S. Shi, Z. Sun, A. Bedoya-Pinto, P. Graziosi, X. Li, X. Liu, L. Hueso, V. A. Dediu, Y. Luo, and M. Fahlman, Adv. Funct. Mater. **24**, 4812 (2014).
[14] A. Bedoya-Pinto, S. G. Miralles, S. Vélez, A. Atxabal, P. Gargiani, M. Valvidares, F. Casanova, E. Coronado, and L. E. Hueso, Adv. Funct. Mater. **28**, 1702099 (2018).
[15] Z. G. Yu, Phys. Rev. B **77**, 205439 (2008).
[16] J. Rybicki and M. Wohlgenannt, Phys. Rev. B **79**, 153202 (2009).
[17] J. Rybicki, T. Nguyen, Y. Sheng, and M. Wohlgenannt, Synth. Met. **160**, 280 (2010).
[18] A. Norambuena, E. Muñoz, H. T. Dinani, A. Jarmola, P. Maletinsky, D. Budker, and J. R. Maze, Phys. Rev. B **97**, 094304 (2018).
[19] R. J. Elliott, Phys. Rev. **96**, 266 (1954).
[20] Y. Yafet, Solid State Phys. **14**, 1 (1963).
[21] C. A. Masmanidis, H. H. Jaffe, and R. L. Ellis, J. Phys. Chem. **79**, 2052 (1975).
[22] Z. G. Yu, Phys. Rev. Lett. **106**, 106602 (2011).
[23] Z. G. Yu, Phys. Rev. B **85**, 115201 (2012).
[24] Z. G. Yu, Nanoelectron. Spintron. **1**, 1 (2015).
[25] M. Cox, E. H. M. van der Heijden, P. Janssen, and B. Koopmans, Phys. Rev. B **89**, 085201 (2014).
[26] M. Kimata, D. Nozaki, Y. Niimi, H. Tajima, and Y. C. Otani, Phys. Rev. B **91**, 224422 (2015).
[27] X. Zhang, S. Mizukami, Q. Ma, T. Kubota, M. Oogane, H. Naganuma, Y. Ando, and T. Miyazaki, J. Appl. Phys. **115**, 172608 (2014).

[28] T. L. Keevers and D. R. McCamey, J. Magn. Reson. **257**, 70 (2015).
[29] J. Rawson, P. J. Angiolillo, P. R. Frail, I. Goodenough, and M. J. Therien, J. Phys. Chem. B **119**, 7681 (2015).
[30] S. Liang, R. Geng, B. Yang, W. Zhao, R. Chandra Subedi, X. Li, X. Han, and T. D. Nguyen, Sci. Rep. **6**, 19461 (2016).
[31] N. J. Harmon and M. E. Flatté, Phys. Rev. Lett. **110**, 176602 (2013).
[32] N. J. Harmon and M. E. Flatté, Phys. Rev. B **90**, 115203 (2014).
[33] S. W. Jiang, S. Liu, P. Wang, Z. Z. Luan, X. D. Tao, H. F. Ding, and D. Wu, Phys. Rev. Lett. **115**, 086601 (2015).
[34] A. V. Shumilin and V. V. Kabanov, Phys. Rev. B **92**, 014206 (2015).
[35] A. Droghetti, I. Rungger, M. Cinchetti, and S. Sanvito, Phys. Rev. B **91**, 224427 (2015).
[36] V. V. Mkhitaryan and V. V. Dobrovitski, Phys. Rev. B **95**, 214204 (2017).
[37] N. Lu, N. Gao, L. Li, and M. Liu, Phys. Rev. B **96**, 165205 (2017).
[38] K. Bader, M. Winkler, and J. van Slageren, Chem. Commun. **52**, 3623 (2016).
[39] G. Breit, Phys. Rev. **34**, 553 (1929).
[40] W. Pauli, Z. Phys. **43**, 601 (1927).
[41] F. Neese and E. I. Solomon, Inorg. Chem. **37**, 6568 (1998).
[42] E. van Lenthe, J. G. Snijders, and E. J. Baerends, J. Chem. Phys. **105**, 6505 (1996).
[43] P. A. M. Dirac, Proc. R. Soc. A Math. Phys. Eng. Sci. **117**, 610 (1928).
[44] M. Douglas and N. M. Kroll, Ann. Phys. (N. Y). **82**, 89 (1974).
[45] B. A. Hess, Phys. Rev. A **32**, 756 (1985).
[46] A. J. Cohen, P. Mori-Sánchez, and W. Yang, Science **321**, 792 (2008).
[47] M. Ernzerhof and G. E. Scuseria, J. Chem. Phys. **110**, 5029 (1999).
[48] D. J. D. Wilson, C. E. Mohn, and T. Helgaker, J. Chem. Theory Comput. **1**, 877 (2005).
[49] F. Neese, J. Chem. Phys. **115**, 11080 (2001).
[50] C. J. Cramer and D. G. Truhlar, Phys. Chem. Chem. Phys. **11**, 10757 (2009).
[51] J. P. Perdew, K. Burke, and M. Ernzerhof, Phys. Rev. Lett. **77**, 3865 (1996).
[52] C. Adamo and V. Barone, Chem. Phys. Lett. **298**, 113 (1998).
[53] J. P. Perdew and Y. Wang, Phys. Rev. B **45**, 13244 (1992).
[54] J. Heyd, G. E. Scuseria, and M. Ernzerhof, J. Chem. Phys. **118**, 8207 (2003).
[55] A. V. Krukau, O. A. Vydrov, A. F. Izmaylov, and G. E. Scuseria, J. Chem. Phys. **125**, 224106 (2006).
[56] P. Rivero, I. P. R. Moreira, G. E. Scuseria, and F. Illas, Phys. Rev. B **79**, 245129 (2009).
[57] R. Gillen, S. J. Clark, and J. Robertson, Phys. Rev. B **87**, 125116 (2013).
[58] M. Valiev, E. J. Bylaska, N. Govind, K. Kowalski, T. P. Straatsma, H. J. Van Dam, D. Wang, J. Nieplocha, E. Apra, T. L. Windus, and W. A. De Jong, Comput. Phys. Commun. **181**, 1477 (2010).
[59] D. A. Pantazis, X.-Y. Chen, C. R. Landis, and F. Neese, J. Chem. Theory Comput. **4**, 908 (2008).
[60] Z. G. Yu, F. Ding, and H. Wang, Phys. Rev. B **87**, 205446 (2013).
[61] S. Watanabe, K. Ando, K. Kang, S. Mooser, Y. Vaynzof, H. Kurebayashi, E. Saitoh, and H. Sirringhaus, Nat. Phys. **10**, 308 (2014).
[62] M. Cinchetti, K. Heimer, J.-P. Wüstenberg, O. Andreyev, M. Bauer, S. Lach, C. Ziegler, Y. Gao, and M. Aeschlimann, Nat. Mater. **8**, 115 (2009).
[63] M. Atzori, L. Tesi, E. Morra, M. Chiesa, L. Sorace, and R. Sessoli, J. Am. Chem. Soc. **138**, 2154 (2016).
[64] M. Atzori, L. Tesi, S. Benci, A. Lunghi, R. Righini, A. Taschin, R. Torre, L. Sorace, and R. Sessoli, J. Am. Chem. Soc. **139**, 4338 (2017).
[65] S. Heutz, C. Mitra, W. Wu, A. J. Fisher, A. Kerridge, M. Stoneham, A. H. Harker, J. Gardener, H.-H. Tseng, T. S. Jones, C. Renner, and G. Aeppli, Adv. Mater. **19**, 3618 (2007).
[66] W. Wu, A. Kerridge, A. H. Harker, and A. J. Fisher, Phys. Rev. B **77**, 184403 (2008).
[67] L. Tesi, A. Lunghi, M. Atzori, E. Lucaccini, L. Sorace, F. Totti, and R. Sessoli, Dalton Trans. **45**, 16635 (2016).
[68] L. Schulz, M. Willis, L. Nuccio, P. Shusharov, S. Fratini, F. L. Pratt, W. P. Gillin, T. Kreouzis, M. Heeney, N. Stingelin, C. A. Stafford, D. J. Beesley, C. Bernhard, J. E. Anthony, I. McKenzie, J. S. Lord, and A. J. Drew, Phys. Rev. B **84**, 085209 (2011).
[69] L. Nuccio, M. Willis, L. Schulz, S. Fratini, F. Messina, M. D'Amico, F. L. Pratt, J. S. Lord, I. McKenzie, M. Loth, B. Purushothaman, J. Anthony, M. Heeney, R. M. Wilson, I. Hernández, M. Cannas, K. Sedlak, T. Kreouzis, W. P. Gillin, C. Bernhard, and A. J. Drew, Phys. Rev. Lett. **110**, 216602 (2013).
[70] J. Hachmann, R. Olivares-Amaya, S. Atahan-Evrenk, C. Amador-Bedolla, R. S. Sánchez-Carrera, A. Gold-Parker, L. Vogt, A. M. Brockway, and A. Aspuru-Guzik, J. Phys. Chem. Lett. **2**, 2241 (2011).
[71] B. Huskinson, M. P. Marshak, C. Suh, S. Er, M. R. Gerhardt, C. J. Galvin, X. Chen, A. Aspuru-Guzik, R. G. Gordon, and M. J. Aziz, Nature (London) **505**, 195 (2014).
[72] U. Chopra, S. A. Egorov, J. Sinova, and E. R. McNellis, J. Phys. Chem. C **123**, 19112 (2019).